arXiv:1909.06056v3 [quant-ph] 21 Aug 2022

Information scrambling and redistribution of quantum correlations through dynamical evolution in spin chains

Saikat Sur[1*] and V. Subrahmanyam[2]

[1*]Department of Chemical and Biological Physics, Weizmann Institute of Science, Rehovot, 7610001, Israel.
[2]School of Physics, University of Hyderabad, Hyderabad, 500046, India.

*Corresponding author(s). E-mail(s): saikat.sur@weizmann.ac.il;
Contributing authors: vmanisp@uohyd.ac.in;

Abstract

We investigate the propagation of local bipartite quantum correlations, along with the tripartite mutual information to characterize the information scrambling through dynamical evolution of spin chains. Starting from an initial state with the first pair of spins in a Bell state, we study how quantum correlations spread to other parts of the system, using different representative spin Hamiltonians, viz. the Heisenberg Model, a spin-conserving model, the transverse-field XY model, a non-conserving but integrable model, and the kicked Harper model, a spin conserving but noninte- grable model. We show that the local correlations spread consistently in the case of spin-conserving dynamics in both integrable and nonintegrable cases, with a strictly nonnegative tripartite mutual information. In contrast, in the case of nonconserving dynamics, tripartite mutual information is negative and local pair correlations do not propagate.

Keywords: Quantum correlations, Information scrambling, Spin chains, Entanglement, Tripartite Mutual information, Hamiltonian Dynamics

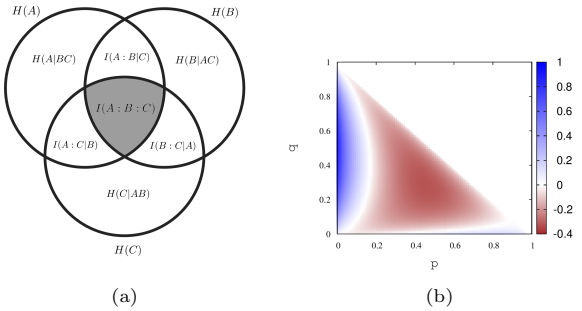
1 Introduction

Quantum entanglement and information in the ground state and the dynamics of quantum spin chains have been extensively studied over the last few years, as spin chains are perceived to be possible channels for quantum communication and information processing. Traditionally, quantum spin chains have been investigated from the view point of quantum state and entanglement transfer [1–5], studying low-dimensional condensed matter physics systems exhibiting quantum phase transitions and a variety of spin orderings [6–10]. These systems have also been studied in the context of the dynamics of quantum many-body systems, for magnon bound and scattering states [11–13], spin current dynamics [14] and relativistic density-wave dynamics [15]. The unitary evolution of quantum correlations, using model Hamiltonians, has been investigated in various fields, e.g., quantum quench dynamics [16–18], the light-cone entanglement spreading [19–21], dynamics of disordered systems [22, 23].

In the last few years, scrambling of quantum information has been investigated in various contexts, for example, in information paradox in black holes [24, 25], in many-body disordered systems [27], in understanding the dynamics of ergodic and integrable systems [28–30]. Now, scrambling of information is quantified by an observable independent quantity called tripartite mutual information (TMI) [31, 32], a combination of bipartite and tripartite quantum correlation functions. It is interesting to investigate the connection between TMI, that is the information scrambling, with the bipartite quantum correlations in a dynamical many-body system. Since the dynamical evolution of the spin chain is through a Hamiltonian evolution, the symmetry property of the spin Hamiltonian and the integrability of the underlying dynamics are expected to play a significant role on the scrambling nature of the dynamics. In this paper, we will address these by studying the dynamics of multi-qubit states initialized with a locally encoded information or an entangled pair. We will be investigating the dynamics of TMI and connect it with the dynamics of two popular bipartite quantum correlation functions, the concurrence measure of quantum entanglement and the quantum mutual information.

We use different spin models, spin conserving or spin non-conserving, integrable or nonintegrable, for the spin chain dynamics. We study the Heisenberg model, that exhibits a spin-conserving dynamics, the XY model in a transverse field with a spin non-conserving dynamics and the kicked Harper model with a non-integrable but spin-conserving dynamics. We investigate how the entanglement is generated and distributed over various pairs of qubits, by studying the time dependence of concurrence measure of pairwise entanglement and pairwise quantum mutual information. The time evolution of tripartite mutual information can be used for each of these cases to categorize the dynamics of spin chains on the basis of their scrambling behaviour, and the relationship between propagation of bipartite correlations and scrambling of information. This paper is organised as follows. We discuss measures of bipartite correlations and scrambling of quantum information, that involves one-party, two-party and three-party correlation functions in section 2. We study the time evolution

of one-magnon and two-magnon initial states and their correlation dynamics, for the Heisenberg model, the kicked Harper model and the transverse-field XY model and the corresponding dynamics of TMI in section 3.



(a) (b)

Fig. 1 (a) The information diagram for three classical variables A, B and C with the shaded region denoting the tripartite mutual information $I(A : B : C)$. (b) The density plot of the tripartite mutual information $I(1 : 2 : 3)$ between three spins for the state given in Eq. 7 as a function of p and q.

2 Quantum correlations and scrambling of quantum information

We briefly review a few popular measures of quantum correlations and information that have been extensively studied for spin systems over the last two decades. The pairwise entanglement and the mutual information will depend on two-point correlation functions. The two-qubit reduced density matrix ρ_{AB} of two qubits A and B is computed by tracing out all other qubits from the full system. In general, for a many-body system, the two-qubit state ρ_{AB} will be a mixed state. The dynamics, for all the models that we will be considering below, conserves the parity, which implies that the elements of the reduced density matrix between two states with odd and even number of up (down) spins are zero.

Let us consider σ^z - diagonal basis states, $|00\rangle$, $|01\rangle$, $|10\rangle$, $|11\rangle$, for two qubits. The two-qubit reduced density matrix ρ_{AB} has the X-state form, given as

$$\rho_{AB} = \begin{pmatrix} u & 0 & 0 & z \\ 0 & w_1 & x & 0 \\ 0 & x^* & w_2 & 0 \\ z^* & 0 & 0 & v \end{pmatrix} \tag{1}$$

The above matrix elements are related to two-point diagonal and off-diagonal correlation functions [33]. For spin-conserving models, like the Heisenberg dynamics, the off-diagonal matrix element z is zero if the initial state has a definite number of down (up) spins, as states with different down spins do not mix. For spin non-conserving transverse-field XY model, the matrix element z can be nonzero [35]. The pairwise concurrence, between two marked qubits, quantifies their mutual entanglement, that takes the value of unity when they are maximally entangled and zero when they are separable. The concurrence [34] measure is defined as,

$$C = \max\{0, \sqrt{\lambda_1} - \sqrt{\lambda_2} - \sqrt{\lambda_3} - \sqrt{\lambda_4}\}. \tag{2}$$

Here, λ_i are eigenvalues of the matrix $\rho_{AB}\tilde{\rho}_{AB}$ in decreasing order, where $\tilde{\rho}_{AB}$ is the time reversed state, given by $\tilde{\rho}_{AB} = (\sigma_A^y \otimes \sigma_B^y)\rho_{AB}^*(\sigma_A^y \otimes \sigma_B^y)$. The concurrence between two qubits, in terms of the two qubit RDM elements is given by the following form [2],

$$C = 2\ \max\{0, |x| - \sqrt{uv}, |z| - \sqrt{w_1 w_2}\}. \tag{3}$$

The quantum mutual information for two parties A and B in the quantum state ρ_{AB}, is defined in terms of the von Neumann entropies $S(\rho_A)$ and $S(\rho_B)$ and $S(\rho_{AB})$ (where $S(\rho) = -Tr\rho\log_2\rho$), given by

$$I(A:B) = S(\rho_A) + S(\rho_B) - S(\rho_{AB}). \tag{4}$$

Unlike the concurrence measure, the mutual information is related to the eigenvalues of the single and the two-qubit reduced density matrices. By the concavity property of von Neumann entropy the mutual information is a non-negative quantity and bounded between 0 and 2. Clearly, the mutual information is zero for pure bipartite factorizable states, as both the composite-system states and the states of its sub-parts are pure and there is no loss of information in accessing the composite system locally. where we can have entanglement within pure states.

Before discussing tripartite mutual information for quantum systems in detail, let us briefly outline the concept of tripartite mutual information in classical information theory. If A, B and C are three random variables, the TMI $I(A:B:C)$ is defined as [26],

$$I(A:B:C) = I(A:B) + I(A:C) - I(A:BC). \tag{5}$$

TMI is not necessarily non-negative unlike the case of mutual information with two variables. The value of $I(A:B:C)$ between three classical variables A, B and C is -1 if B and C are independent random variables and $A = B \oplus C$. In this case, the information shared between the random variables A and BC jointly is larger than the informations shared between the random variables A and B; A and C jointly. The value of $I(A:B:C)$ between them is 1 if they

all are identical, i.e., $A = B = C$. On the other hand, $I(A : B : C) = 0$ if all the variables A, B and C are independent and random.

In the context of quantum dynamics, the locally-encoded quantum information spreads out over the entire system through a unitary time evolution. Such delocalization of quantum information is referred to as scrambling [24, 25, 27, 31, 32]. This implies that local disturbances in the initial states cannot be detected by local measurements on the output states if scrambling of information occurs. Let us consider a system consisting of three subparts A, B and C. In this case, a local measurement on a subpart A may not reveal much information about a local disturbance at a different subpart B if scrambling occurs. Therefore, the mutual information $I(A : B)$ would be small. From a similar reasoning, the pairwise mutual information $I(A : C)$ also would be small. The mutual information $I(A : BC)$ quantifies the total amount of information one can learn about A by measuring the part BC jointly. Since one is interested in the amount of information concerning A, which is hidden nonlocally over B and C, a measure of scrambling would be given by the quantity known as tripartite mutual information (TMI) [31, 32]. This is a measure to quantify by how much the information shared by A with B and C together is different from the sum of the informations shared pairwise by A with B, and by A with C. Using the definition of the mutual information given in Eq. 4, one can rewrite the expression fot TMI in terms of the von Neumann entropies of one, two and three-party reduced density matrices, symmetric in the labels A, B, and C as

$$I(A : B : C) = S(\rho_A) + S(\rho_B) + S(\rho_C) - S(\rho_{AB}) - S(\rho_{BC}) - S(\rho_{CA}) + S(\rho_{ABC}). \tag{6}$$

If ρ_{ABC} represents a pure state, for any partition between the subparts A and BC, the two parts will have the same von Neumann entropy, i.e., $S(\rho_A) = S(\rho_{BC})$, and similarly for other bi-partitions. Thus, the tripartite mutual information is identically zero. But it becomes a non-trivial measure for a tripartite mixed state or a many-qubit pure state with at least four qubits. A positive TMI implies that A with B and A with C share some redundant information as compared to A with BC. In this case, quantum correlations and information between two parties $A - B$ and $A - C$ propagate to other qubits in a many-qubit system through further time evolution as a form of bipartite correlations. On the other hand, a negative TMI implies that the sum of information shared between A and B ; A and C is smaller than that between A and BC together, signifying that a fraction of quantum correlations are delocalized in the form of correlations among three or more parties as opposed to local two-party correlations. As a consequence, this delocalized information do not propagate as bipartite correlations through further time evolution with a finite speed through the system. This is a signature for the loss of information, and hence scrambling of information. Evidently, the more the negative TMI is, the more is the delocalization of bipartite correlations.

To illustrate the scrambling of information and TMI, let us consider a few representative states. For a four-qubit pure state of the form, $|\psi\rangle = |\phi\rangle_1 \otimes |\phi\rangle_{234}$, we have $I(1:2:3) = 0$, where 1 and 234 are not entangled. For the four-qubit GHZ-like state, $|\psi\rangle = (|0000\rangle + |1111\rangle)/\sqrt{2}$ has $I(1:2:3) = 1$ for any three qubits. For the four-qubit W-state $|\psi\rangle = (|1000\rangle + |0100\rangle + |0010\rangle + |0001\rangle)/2$ has $I(1:2:3) \sim 0.244$ for any three qubits. Now, to illustrate that TMI can be negative, let us consider a simple three-qubit mixed state given as,

$$\rho = p\frac{1}{3}|100 + 010 + 001\rangle\langle 100 + 010 + 001| + q|111\rangle\langle 111| + (1 - p - q)|000\rangle\langle 000|, \tag{7}$$

where, $p, q \geq 0$ and $p + q \leq 1$. For this state the tripartite mutual information is straightforward to compute, and shown as a density plot in Fig. 1(b) as a function of p and q. For the cases $p = 0$, $q = 1$ and $p = 1$, $q = 0$ the state ρ is a pure three qubit state and $I(1:2:3)$ becomes zero as evident from its definition. The sign of $I(1:2:3)$ depends on the values of p and q in the rest of the region. For instance, we can see that the tripartite mutual information for this state is negative for $p \gtrsim 0.2$.

3 Dynamical evolution of local quantum correlations in various spin models

We now consider the dynamical evolution of an initial spin state using Hamiltonian dynamics. Through the time-evolution, a variety of spin correlations can be dynamically generated from a locally correlated initial state. We explicitly study below, three model spin Hamiltonians: the anisotropic Heisenberg Hamiltonian, an integrable and spin-conserving model, the periodically kicked Harper model, a nonintegrable but spin-conserving model, and the transverse field XY model, an integrable but spin non-conserving model. The propagation of a signal of quantum dynamical process and interference with the state transfer have been investigated for these models [36, 37], where it was seen that a finite speed of propagation cannot be defined for nonintegrable dynamics. We will see below that the consistent spreading of local quantum correlations does not depend on non-integrability, but depends significantly on whether the dynamics is spin conserving or not.

3.1 Anisotropic Heisenberg model

We consider first an exactly-solvable and integrable non-trivial model of interacting quantum spins in a one dimensional array, interacting with nearest-neighbour Heisenberg exchange interaction. Using the Pauli matrices $\vec{\sigma}_i$ to represent the different components of the spin operator at the ith site, the anisotropic Heisenberg Hamiltonian for a one-dimensional chain of N spins is

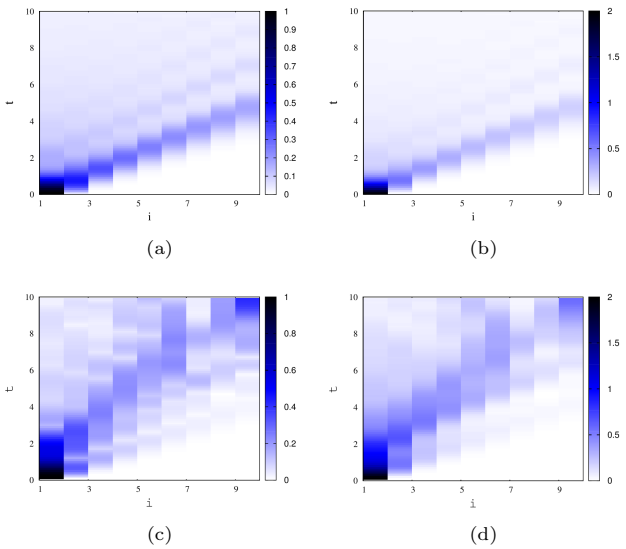


Fig. 2 The time dependence of the concurrence and the mutual information between the sites i and $i+1$ as functions of time t for the Heisenberg model: (a) the concurrence, (b) the mutual information for the initial state $|10...0+010...0\rangle/\sqrt{2}$, (c) the concurrence, (d) the mutual information for the initial state $|00...0+110...0\rangle/\sqrt{2}$. The anisotropy constant is $\Delta = 1.0$.

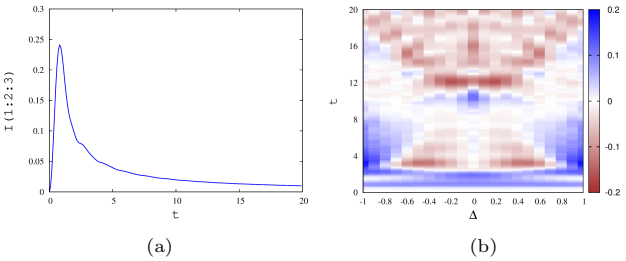


Fig. 3 The time dependence of TMI $I(1:2:3)$ for anisotropic Heisenberg model for the initial states (a) $|01...0+100...0\rangle/\sqrt{2}$ and (b) $|00...0+110...0\rangle/\sqrt{2}$ with anisotropy constant Δ with time t.

given by,

$$H = -J\sum_i(\sigma_i^x\sigma_{i+1}^x + \sigma_i^y\sigma_{i+1}^y + \Delta\sigma_i^z\sigma_{i+1}^z), \tag{8}$$

where J is the exchange interaction strength for the nearest-neighbour spins, and Δ is the anisotropy parameter. The model exhibits ferromagnetic behaviour in the ground state for $\Delta \geq 1$. In the region, $-1 < \Delta < 1$, the model is gap-less and is in the spin-liquid phase with a power law decay of correlations. In the region, $\Delta \leq -1$, the ground state shows a Néel long range order. All the eigenstates of this model are known, and can be found using the Bethe Ansatz [10].

Let the basis states for the ith spin be $|0\rangle$ (up-spin state) and $|1\rangle$ (down-spin state), denoting the eigenstates of σ_i^z with eigenvalues $+1$ and -1 respectively. The basis states for the many-qubit system can be chosen to be the direct product states of the basis states of each spin. The z-component of the total spin $\Sigma\sigma_i^z$ is a constant of motion, which implies that the eigenstates will have a definite number of down spins and parity. The many-qubit basis states with l down spins can also be labeled by the locations $(x_1, x_2...x_l)$, where the set is an ordered set with $x_1 < x_2... < x_l$. An eigenstate with l down spins, a l-magnon state, can be written as a superposition of the basis states as,

$$|\psi\rangle = \sum_{x_1,x_2...,x_l} \psi(x_1, x_2...x_l)|x_1, x_2...x_l\rangle, \tag{9}$$

where the eigenfunction $\psi(x_1, x_2..., x_l)$ denotes the wave function amplitude for the basis state $|x_1, x_2..., x_l\rangle$. The eigenfunction is given by the Bethe Ansatz [38], labeled by the set of quasi-momenta $(p_1, p_2...p_l)$ of the down spins, which are determined by solving algebraic Bethe Ansatz equations, with periodic boundary conditions.

There is only one zero-magnon state $|F\rangle = |00...0\rangle$, which is just a ferromagnetic ground state with all the spins polarized along one direction. It is straightforward to see that it is an eigenstate of the above Hamiltonian with energy $\epsilon_0 = -NJ\Delta$ for periodic boundary conditions. Starting from $|F\rangle$, one-magnon excitations can be created by turning any one of the spins, giving N localized one-magnon states, which can be labeled by the location of the down spin. One-magnon eigenstates are labeled by the momentum p of the down spin, the eigenfunction is given by,

$$\psi_p^x = \sqrt{\tfrac{1}{N}} e^{ipx};\ p = \tfrac{2\pi I}{N}, \text{for a closed chain} \tag{10}$$

where the momentum p is determined by an integer $I = 1, 2, ...N$. The one-magnon eigenvalue is given by $\epsilon_1(p) = \epsilon_0 - 2J\cos p$. The interaction strength J determines the hopping of the down spins to neighbouring sites, and the interaction between the two down spins is determined by the anisotropy constant Δ. The one-magnon eigen energies are independent of Δ as the states carry only one down spin.

We will investigate the dynamics of quantum correlations by focusing on the evolution of a locally entangled state. For investigating the effect of a many-body interaction term in the Hamiltonian, we will consider two different initial states, a one-magnon entangled state and an entangled state in the zero and two-magnon subspace. The one-magnon eigenstates are not affected by the many body interaction term in the Hamiltonian, but the pair entanglement spreads out as the down spin moves around. The anisotropy parameter Δ plays a role in the case of the two-magnon state.

Let us first consider an initial state that is a linear combination of localized one-magnon states, given by

$$|\Psi(0)\rangle = \alpha|100...0\rangle + \beta|010...0\rangle = \alpha|1\rangle + \beta|2\rangle. \tag{11}$$

Here, we have written the initial state as a superposition of states with the down spin is at sites 1 and 2. Through the time evolution the down spin moves due to the interaction. The time evolution of the state is straightforward, the state after a time t becomes,

$$|\Psi(t)\rangle = \sum_x \Omega^x(t)|x\rangle, \tag{12}$$

where the time dependent function $\Omega^x(t)$ is given in terms of one particle Green functions [2, 36] in the following form,

$$\Omega^x(t) = \alpha G_1^x(t) + \beta G_2^x(t). \tag{13}$$

The time-dependent function $G_x^{x'}(t)$ [2] is given in terms of the wave functions defined above as,

$$G_x^{x'}(t) = \sum_p \psi_p^x \psi_p^{x'*} e^{-it\epsilon_1(p)}. \tag{14}$$

In the macroscopic limit, $N \to \infty$, the sum over the momentum can be converted into an integral, thus, we get,

$$G_x^{x'}(t) = \frac{1}{2\pi}\int_0^{2\pi} e^{-it\cos p - ip(x-x')}dp = J_{x-x'}(t)i^{x-x'}. \tag{15}$$

The reduced density matrix for the jth qubit can be worked out easily, we have

$$\rho_j = (1-|\Omega^j|^2)|0\rangle\langle 0| + |\Omega^j|^2|1\rangle\langle 1|. \tag{16}$$

The elements of the two-qubit reduced density matrix (as shown in Eq. 1), for the jth and kth qubits, for direct evolution of the states can be calculated from Eq. 12 and Eq. 13,

$$u_{j,k} = 1-|\Omega^j|^2-|\Omega^k|^2,\ w_{1\,j,k} = |\Omega^k|^2,\ w_{2_{j,k}} = |\Omega^j|^2,\ x_{j,k} = \Omega^{j*}\Omega^k. \tag{17}$$

The other elements of the reduced density matrix are zero for this case. Similarly, one can compute the elements of the three qubit reduced density matrix also. The forms of the elements are cumbersome to present here, so instead we directly present the expression for the TMI for three qubits. For the three marked qubits j, k and l, TMI can be expressed in terms of the two-body correlation functions given in Eq. 17, and the Shannon binary entropy $H(x) = -x\log_2 x - (1-x)\log_2(1-x)$, as

$$I(j:k:l) = \sum_{p=j,k,l} H\left(|\Omega^p|^2\right) + \sum_{p,q=j,k,l} H\left(|\Omega^p|^2 + |\Omega^q|^2\right) + H\left(|\Omega^j|^2 + |\Omega^k|^2 + |\Omega^l|^2\right). \tag{18}$$

Here, the quantities $|\Omega^j|^2, |\Omega^k|^2$, and $|\Omega^l|^2$ are clearly non negative fractions, implying that $I(j:k:l)$ is non negative, as shown in Fig. 3(a). Thus, the scrambling of information does not occur in this case.

Let us now consider an initial state that is an entangled state in zero and two magnon subspace, given as

$$|\Psi(0)\rangle = \alpha|0...0\rangle + \beta|110...0\rangle = \alpha|F\rangle + \beta|1,2\rangle. \tag{19}$$

The time evolution of the state is straightforward, the state after a time t becomes,

$$|\Psi(t)\rangle = \alpha e^{-i\epsilon_0 t}|F\rangle + \sum_{x_1,x_2} G_{1,2}^{x_1,x_2}(t)|x_1,x_2\rangle, \tag{20}$$

The details of the two-particle time-dependent Green function $G_{1,2}^{x_1,x_2}(t)$ is discussed in [37]. The two-particle Green's function is defined in terms of the two-magnon eigenfunctions $\psi_{p_1,p_2}(x_1,x_2)$, and the eigenvalues $\epsilon_2(p_1,p_2)$, we have,

$$G_{x_1,x_2}^{x_1',x_2'}(t) = \sum_{p_1,p_2} \psi_{p_1,p_2}^{x_1,x_2} \psi_{p_1,p_2}^{x_1',x_2'*} e^{-it\epsilon_2(p_1,p_2)}. \tag{21}$$

The elements of the one and two-qubit reduced density matrix for direct evolution of the states can be calculated from Eq. 20. The reduced density matrix for the jth qubit is given as,

$$\rho_j = (1-|\beta|^2 \sum_{x;\ x\neq j} |G_{1,2}^{j,x}|^2)|0\rangle\langle 0| + |\beta|^2 \sum_{x;\ x\neq j} |G_{1,2}^{j,x}|^2 |1\rangle\langle 1|. \tag{22}$$

The elements of the reduced density matrix $\rho_{j,k}$ given in Eq. 1 are given as,

$$\begin{aligned}
u_{j,k} &= |\alpha|^2 + |\beta|^2 \sum_{x_1,x_2;\ x_1,x_2\neq j,k} |G_{1,2}^{x_1,x_2}|^2, \\
w_{1\,j,k} &= |\beta|^2 \sum_{x;\ x\neq j} |G_{1,2}^{k,x}|^2, \\
w_{2\,j,k} &= |\beta|^2 \sum_{x;\ x\neq k} |G_{1,2}^{j,x}|^2, \quad x_{j,k} = |\beta|^2 \sum_{x;\ x\neq j,k} G_{1,2}^{j,x} G_{1,2}^{*k,x}, \\
v_{j,k} &= |\alpha|^2, \quad z_{j,k} = \alpha\beta^* e^{-i\epsilon_0 t} G_{1,2}^{*j,k}.
\end{aligned} \tag{23}$$

The two particle Green functions $G_{1,2}^{x_1,x_2}$ have been calculated numerically for different values of anisotropy constant Δ. Accordingly, the three-qubit

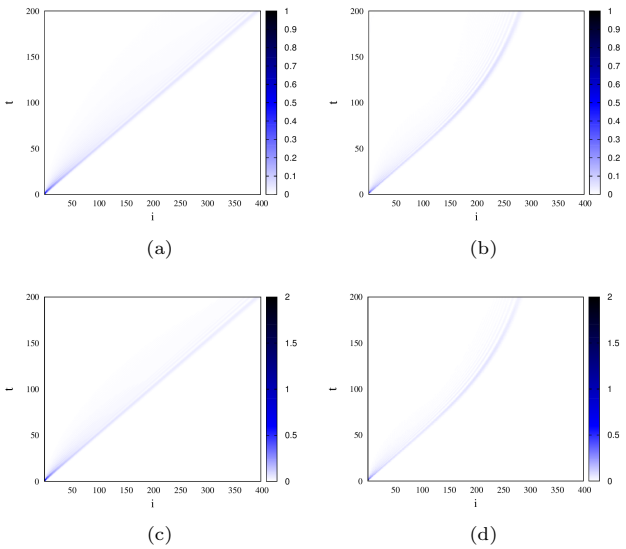


Fig. 4 The time dependence of the concurrence and the mutual information between the sites i and $i+1$ for the Harper model: The concurrence is shown for parameters (a) $g = 0.1, \tau = 0.1$, (b) $g = 1.0, \tau = 0.9$. The mutual Information is shown for parameters (c) $g = 0.1, \tau = 0.1$, (d) $g = 1.0, \tau = 0.9$. The results are shown for the initial state $|10...0 + 010...0\rangle/\sqrt{2}$.

reduced density matrix $\rho_{j,k,l}$ for three qubits j, k and l has been calculated in order to compute the TMI. We illustrate the results for the initial states with a Bell pair at the first two spins i.e., $(|10...0\rangle + |010...0\rangle)/\sqrt{2}$ and $(|00...0\rangle + |110...0\rangle)/\sqrt{2}$. The nearest neighbour concurrence $C(i, i+1)$, mutual information $I(i, i+1)$ are plotted as functions of time t and site index i in Fig. 2(a) and 2(b) for the initial state $|\Psi(0)\rangle = \frac{1}{\sqrt{2}}(|10...0\rangle + |010...0\rangle)$ and in Fig. 2(c) and 2(d) for the initial state $|\Psi(0)\rangle = \frac{1}{\sqrt{2}}(|00...0\rangle + |110...0\rangle)$ respectively for the anisotropic Heisenberg model. Both the concurrence and the mutual information are monotonic and show similar features. The pairwise entanglement and the correlations moves linearly in time as time evolves from the first two sites to the rest of the chain.

Tripartite mutual information $I(1:2:3)$ is plotted as a function of time t for the initial state $(|100...0\rangle + |010...0\rangle)/\sqrt{2}$ in Fig. 3(a) and for different values of the anisotropic parameter Δ in Fig. 3(b) respectively. Unlike for the initial state in one magnon subspace, we see here that the matrix element z of two-qubit reduced density matrix is non zero indicating the mixing between the zero and the two magnon sectors. As a result, the TMI can be negative despite the dynamics being spin-conserving. The scrambling is very small as the minimum value of TMI is around -0.2.

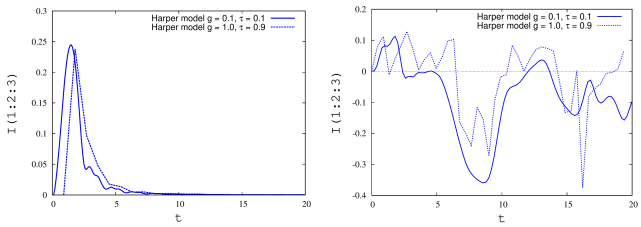


Fig. 5 The time dependence of TMI $I(1:2:3)$ for the Kicked Harper model with different set of parameters $\tau = 0.1, g = 0.1$ and $\tau = 0.9, g = 1.0$ as a function of time t.

3.2 Periodically Kicked Harper model

Next, we consider a simple model Hamiltonian with a tunable parameter, to go continuously from a completely integrable to a completely non-integrable regime. We use a one-dimensional periodically-kicked Harper model, a simple model of fermions hopping on a chain with an inhomogeneous site potential, appearing as a kick at regular intervals. The spin operator version of the Hamiltonian is given by

$$H(t) \;= \sum_{j=1}^{N}[-\frac{1}{2}(\sigma_j^x\sigma_{j+1}^x + \sigma_j^y\sigma_{j+1}^y) + g\sum_{n=-\infty}^{\infty}\delta(\frac{t}{\tau} - n)\cos(\frac{2\pi j\eta}{N})\sigma_j^z]. \quad (24)$$

The first term is the XY term of the Heisenberg model considered above, that causes hopping of up or down spins. The last term is an inhomogeneous magnetic field in the transverse direction that comes into play through kicks at an interval of τ. The coupling strength g and the kicking interval τ can be independently varied, that can affect the nature of the dynamics as we will see below.

The classical version of the kicked Harper Hamiltonian is regular for $\tau \to 0$ and completely chaotic for large values of τ, and similarly, the eigenvalues and the eigenfunctions of the quantum version display correspondingly a regular or a chaotic characteristics [39–41]. We consider evolution at discrete times, viz., $t = \tau^+, 2\tau^+$ etc, i.e. at instants just after a kick. The unitary operator for the evolution between two kicks is straightforwardly given by,

$$U(g,\tau) = e^{-i\tau\sum_j -\frac{1}{2}(\sigma_j^x\sigma_{j+1}^x + \sigma_j^y\sigma_{j+1}^y)}e^{-i\tau g\sum_j \cos\frac{2\pi j\eta}{N}\sigma_j^z}, \quad (25)$$

where, the two operator factors appearing above do not commute. The time evolved state at time $n\tau^+$ just after n kicks is $|\Psi(t)\rangle = U^n(g,\tau)|\Psi(0)\rangle$. The system evolves between two kicks at $n\tau^+$ and $(n+1)\tau^-$ through the XY dynamics but kicks introduce a lattice position dependent phase factor to the Green function. We consider the initial state $|\Psi(0)\rangle = \alpha|10...0\rangle + \beta|010...0\rangle$ of

the system and the time evolved state will be given by,

$$|\tilde{\Psi}(t = n\tau^+)\rangle = \sum_x \tilde{\Omega}^x(t = n\tau)|x\rangle, \tag{26}$$

where, $\tilde{\Omega}^x(t = n\tau) = \sum_x \alpha \tilde{G}_1^x(t = n\tau)|x\rangle + \beta \tilde{G}_2^x(t = n\tau)|x\rangle$.

Here we have introduced a composite Green function [37, 41], related to the Green function studied in the Heisenberg dynamics, given in the following form,

$$\tilde{G}_{x_0}^{x_n}(t = n\tau) = \sum_{x_1, x_2, \ldots, x_n} \prod_{j=0}^{n-1} G_{x_j}^{x_{j+1}}(\tau) e^{2i\tau g \cos(\frac{2\pi\eta x_{j+1}}{N})}. \tag{27}$$

It can be seen that after each kick, a site-dependent new phase is introduced in the Green function which indicates a qualitative change in the dynamics from the previously discussed Heisenberg dynamics. By setting $g\tau = 0$ in the above, the composite Green function $\tilde{G}_1^x(t)$ reduces to the Green function $G_1^x(t)$, the one-magnon Green function of the Heisenberg model. The form of the reduced density matrices will remain unchanged as given in Eq. 16 and Eq. 17. Let us first consider the initial state given in Eq. 11, a linear combination of one magnon states. Since the system here is non-interacting, the time-dependent wave function from any initial state can be written as a product of the Green function given in Eq. 27. The form of the two qubit RDM derived for the Heisenberg dynamics with one magnon states in Eq. 17 is also valid for the Harper dynamics with the composite Green function.

The nearest neighbour concurrence $C(i, i+1)$ and the mutual information $I(i, i+1)$ are plotted for two representative values of τ and g as functions of site index i and time t for the kicked Harper model in Fig. 4(a)- 4(b). The pairwise concurrence and the mutual information moves from the first pair to large distances with time. For $\tau = 0.1$ and $g = 0.1$ the dynamics resembles the Heisenberg dynamics, where correlations spread linearly as seen in Fig. 4(a) and 4(c). But for $\tau = 0.9$ and $g = 1.0$, the light cone structure becomes non linear as seen in Fig. 4(b) and 4(d). Even in this regime, the dynamics is not much different from the Heisenberg dynamics as the number of magnons is conserved. The correlation dynamics does not change qualitatively for large values of $g\tau$, where the dynamics is nonintegrable. The TMI of the first three qubits $I(1:2:3)$ has been plotted for the kicked Harper model for both the cases $\tau = 0.1, g = 0.1$ and $\tau = 0.9, g = 1.0$ for the initial state $|\Psi(0)\rangle = (|100...0\rangle + |010...0\rangle)/\sqrt{2}$. As shown in Fig. 5(a), the quantity $I(1:2:3)$ is non negative for all the cases. One can also argue this from Eq. 18 that TMI is non-negative when the dynamics is spin-conserving and confined to a one magnon sector. For the initial state $|\Psi(0)\rangle = (|000...0\rangle + |110...0\rangle)/\sqrt{2}$, the quantity $I(1:2:3)$ can be negative, as shown in Fig. 5(b). Similar to the Heisenberg dynamics, the zero and the two magnon sectors mix as the matrix element z of the two-qubit reduced density matrix is non zero.

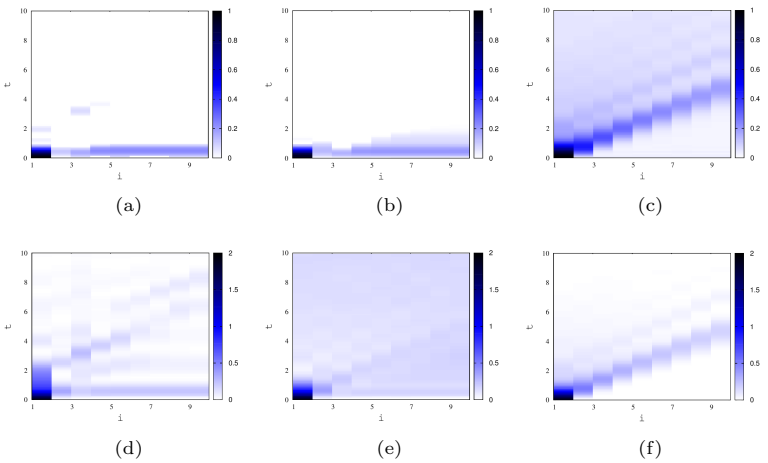


Fig. 6 The concurrence and the mutual information measures between the sites i and $i+1$ as functions of time t for the XY model with a transverse field: The concurrence shown for parameters: (a) $J_x = 0.7, J_y = 0.3$ and $h = 0.1$, (b) $J_x = 0.7, J_y = 0.3$ and $h = 1.0$, (c) $J_x = 0.7, J_y = 0.3$ and $h = 10.0$. The mutual Information for parameters (d) $J_x = 0.7, J_y = 0.3$ and $h = 0.1$, (e) $J_x = 0.7, J_y = 0.3$ and $h = 1.0$, (f) $J_x = 0.7, J_y = 0.3$ and $h = 10.0$. The results are shown from analytical calculations for the initial state: $|\Psi(0)\rangle = (|10...0\rangle + |010...0\rangle)/\sqrt{2}$.

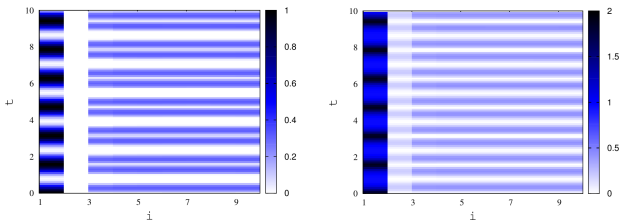


Fig. 7 The concurrence and the mutual information measures are shown between the sites i and $i+1$ as functions of time t for the Ising model: (a) the concurrence, (b) the mutual information. The results are shown from analytical calculations for the initial state $|10...0 + 010...0\rangle/\sqrt{2}$.

Till now we have seen that the qualitative nature of spreading of correlations from a maximally entangled pair or Bell pair does not depend on the integrability of the dynamics. But confinement of the dynamics into a much smaller subspace of the Hilbert space leads to better transfer of quantum correlations in a many body system. As we have seen that bipartite correlations spread to long distances for the Heisenberg model and the kicked Harper model, where the number of down (up) spins is a conserved quantity. So, it can be concluded that spreading of bipartite quantum correlations in a quantum many-body system is associated with a non-negative value of TMI as in the cases of the Heisenberg and the kicked Harper model.

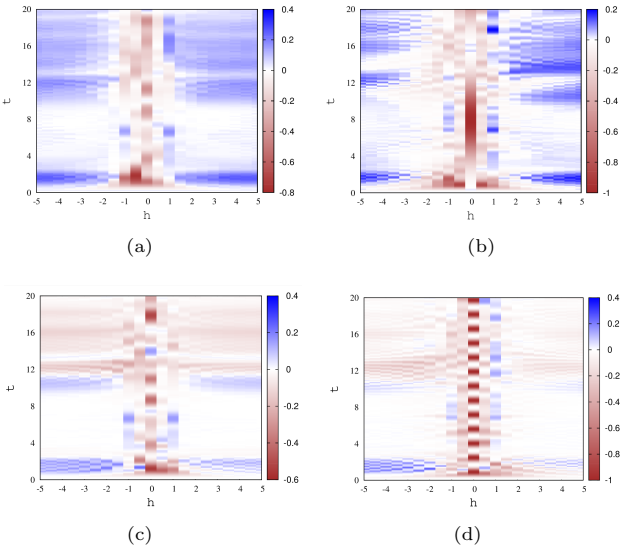


Fig. 8 The time dependence of $I(1:2:3)$ with time: (a) for the XY model ($J_x = 0.7$, $J_y = 0.3$) with different values of transverse magnetic field h, (b) for the Ising model with different values of transverse magnetic field h for the initial state $|10...0 + 010...0\rangle/\sqrt{2}$; (c) for the XY model ($J_x = 0.7$, $J_y = 0.3$) with different values of transverse magnetic field h, (d) for the Ising model with different values of transverse magnetic field h for the initial state $|00...0 + 110...0\rangle/\sqrt{2}$.

3.3 Transverse field XY model

Till now, we have considered model Hamiltonians that conserve the total magnetization. Now, we consider the XY model with a transverse magnetic field, where the dynamics is spin non-conserving. The general Hamiltonian for a one dimensional XY model with N spins with a magnetic field in the transverse direction is given as,

$$H = \sum_i J_x \sigma_i^x \sigma_{i+1}^x + J_y \sigma_i^y \sigma_{i+1}^y + h\sigma_i^z. \tag{28}$$

Here, the periodic boundary condition is assumed. It is easy to see that the three different terms in the above Hamiltonian do not commute with each other for $J_x \neq J_y \neq 0$. The ground state exhibits a quantum critical behaviour, for the isotropic case of $J_x = J_y$ for all values of the magnetic field strength, and for the anisotropic case for $h = J_x + J_y$. Since the spin 1/2 operators are neither bosons nor fermions, the Hamiltonian can be exactly diagonalized and the entire eigenvalue spectrum can be found by employing Jordan-Wigner transformation [7, 8] that maps spin 1/2 operators to spinless fermionic operators. The mapping is given by,

$$\sigma_l^+ = c_l^\dagger e^{i\pi \sum_{m=1}^{l-1} c_m^\dagger c_m}. \tag{29}$$

The Hamiltonian, having a bilinear form in terms of Fermionic creation and annihilation operators, can be brought to a diagonal form by doing a Fourier transformation, followed by a Bogoliubov-Valatin transformation [42, 43]. Fourier transformation maps the operators into momentum space, as follows

$$c_q = \frac{1}{\sqrt{N}} \sum e^{-iql} c_l. \tag{30}$$

Here, the set of allowed momentum values are given by $q = 2\pi m/N$, with $m = -(N-1)/2, ..., -1/2, 1/2, ..., (N-1)/2$ for even values of N; and $m = N/2, ..., 0, ..., N/2$ for odd values of N. In terms of these momentum-space operators the Hamiltonian has a bilinear form with non-diagonal operators $c_q^\dagger c_{-q}^\dagger$ and similar terms.

To diagonalize the Hamiltonian we employ Bogoliubov-Valatin transformation in which new Fermion creation and annihilation operators are formed as a linear combination of old operators,

$$\eta_{1q} = u_q c_q - i v_q c_{-q}^\dagger, \quad \eta_{2q} = -i v_q c_q + u_q c_{-q}^\dagger. \tag{31}$$

The expansion coefficients and the eigenvalues are given by the following forms,

$$u_q = \sqrt{\frac{1}{2} + \frac{(J_x + J_y)\cos q + h}{|\omega_q|}}, \quad v_q = \sqrt{1 - u_q^2}, \tag{32}$$

$$\omega_q = 2\sqrt{[(J_x + J_y)\cos q + h]^2 + [(J_x - J_y)\sin q]^2}. \tag{33}$$

In terms of these new fermion operators the Hamiltonian is diagonal and is given as,

$$H = \sum_{0<q<\pi} |\omega_q| (\eta_{1q}^\dagger \eta_{1q} - \eta_{2q}^\dagger \eta_{2q}). \tag{34}$$

The elements of the reduced density matrix, given in Eq. 1, in terms of spin operators and fermion operators are given by,

$$\begin{aligned}
u_{j,k} &= \frac{1 + \langle\sigma_j^z\rangle + \langle\sigma_k^z\rangle + \langle\sigma_j^z\sigma_k^z\rangle}{4} = 1 - \langle c_j^\dagger c_j\rangle - \langle c_k^\dagger c_k\rangle + \langle c_j^\dagger c_j c_k^\dagger c_k\rangle, \\
v_{j,k} &= \frac{1 - \langle\sigma_j^z\rangle - \langle\sigma_k^z\rangle + \langle\sigma_j^z\sigma_k^z\rangle}{4} = \langle c_j^\dagger c_j c_k^\dagger c_k\rangle, \\
w_{1\,j,k} &= \frac{1 - \langle\sigma_j^z\rangle + \langle\sigma_k^z\rangle - \langle\sigma_j^z\sigma_k^z\rangle}{4} = 1 - \langle c_k^\dagger c_k\rangle - \langle c_j^\dagger c_j c_k^\dagger c_k\rangle, \\
w_{2\,j,k} &= \frac{1 + \langle\sigma_j^z\rangle - \langle\sigma_k^z\rangle - \langle\sigma_j^z\sigma_k^z\rangle}{4} = 1 - \langle c_j^\dagger c_j\rangle - \langle c_j^\dagger c_j c_k^\dagger c_k\rangle, \\
x_{j,k} &= \langle\sigma_j^+\sigma_k^-\rangle = \langle c_j c_k^\dagger\rangle \text{ for } k = j+1, \\
z_{j,k} &= \langle\sigma_j^+\sigma_k^+\rangle = \langle c_j c_k\rangle \text{ for } k = j+1.
\end{aligned}$$

(35)

Now, the time evolution of the fermion annihilation operator c_q in the momentum space becomes,

$$c_q(t) = \chi_q(t)\ c_q + \xi_q(t)\ c^\dagger_{-q}, \tag{36}$$

with time dependent functions $\chi_q(t) = (e^{-i\omega_q t}u_q^2 + e^{i\omega_q t}v_q^2)$ and $\xi_q(t) = -\frac{q}{|q|}2u_q v_q \sin\omega_q t$.

Let us consider the following initial state, a linear combination of one down spin states,

$$|\Psi(0)\rangle = \alpha|10...0\rangle + \beta|010...0\rangle = (\alpha c_1^\dagger + \beta c_2^\dagger)\prod_{q>0}|0\rangle_q|0\rangle_{-q}. \tag{37}$$

Time evolution of the state will generate all odd magnon sector states. From the explicit forms of the correlations functions given in Appendix A Eq. A1 we can compute the bipartite measures of quantum correlations as a function of time. The nearest neighbour concurrence $C(i, i+1)$ and the mutual information $I(i, i+1)$ are plotted as functions of site index i and time t for the XY model with a transverse field in Fig. 6. Here also we illustrate our results for the same three sets of Hamiltonian parameters $(J_x = 0.7, J_y = 0.3, h = 0.1)$; $(J_x = 0.7, J_y = 0.3, h = 1.0)$ and $(J_x = 0.7, J_y = 0.3, h = 10.0)$. Unlike the Heisenberg model, the pairwise concurrence from the Bell state does not spread from first two sites for the cases $h = 0.1$ and $h = 1.0$ as shown in Fig. 6(a) and 6(b). Since parity is conserved and the state contains all odd number of down spins, initially the pairwise concurrence is generated but after sometime it decays. Similarly, the pairwise mutual information does not spread from first two sites for the cases $h = 0.1$ and $h = 1.0$ as shown in Fig. 6(d) and 6(e) respectively. However, the spins generate mutual information between them as a result of the dynamics. But only for the case $h = 10.0$, the pairwise concurrence and the mutual information do spread with a finite speed from the first two sites and their values are zero outside the light cone as shown in Fig. 6(c) and 6(f) respectively.

The transverse field XY model reduces to the Ising model when $J_y = 0$ and $h = 0$. In this case the expectation values of the spin correlation functions take simpler and closed forms given in Appendix B Eq. B2. The nearest neighbour concurrence $C(i, i+1)$ and the mutual information $I(i, i+1)$ are plotted as functions of site index i and time t for the Ising model in Fig. 7(a) and 7(b) respectively. Since the Ising dynamics entangles only two neighbour spins, the local bipartite correlations and the entanglement at the first two sites trivially do not spread, and a speed of the correlation propagation cannot be defined. However, pairwise correlations between the spins are generated due to local two qubit entanglement operations.

The time dependence of tripartite mutual information (TMI) for the transverse field XY model and the Ising model has been plotted in Fig. 8. In Fig. 8(a), the quantity $I(1:2:3)$ is plotted as a function of time t and magnetic field h for the XY model with a transverse field for the parameters $J_x = 0.7, J_y = 0.3$. The quantity $I(1:2:3)$ is mostly negative in the range $|h| < 1$ and non negative for large h region. It can also be seen in Fig. 8(b) that $I(1:2:3)$ becomes negative for the Ising model with parameters $J_x = 1.0, J_y = 0.0$ for the magnetic field in the range $|h| < 1$. For the Ising model without a transverse field, the value of the quantity $I(1:2:3)$ is strictly bounded between 0 and -1 implying a perfect scrambling of information. For a higher value of the transverse field $|h| >> 1$, the value is again non negative. So, scrambling mostly takes place in the range $|h| < 1$ for both these two non spin-conserving models. For comprehensiveness of our analysis, the results for the Bell state with zero and two magnon subspace, i.e., $(|00...0\rangle + |110...0\rangle)/\sqrt{2}$ for the transverse field XY model and the Ising model have also been shown in Fig. 8(b) and (c) respectively. Here all even magnon sectors will be generated unlike the one magnon initial state. The result is qualitatively similar to that of the one magnon initial state for the range $|h| < 1$. However, the quantity $I(1:2:3)$ is not strictly non negative in the limit $|h| >> 1$ unlike the one magnon initial state. This can be well understood, as in the said limit, the dynamics is not restricted to the a particular subspace, rather still mixes zero and two magnon sectors. But in both the cases, the scrambling is much more prominent compared to that of the anisotropic Heisenberg model even with the initial state $(|00...0 + |110...0\rangle)/\sqrt{2}$ (Cf. Fig. 3). Therefore, it can be concluded that the confinement and decay of bipartite quantum correlations in local spins is associated with a high negative value of TMI as seen in the cases of the Ising model and the XY model with a small magnetic field.

4 Conclusions

We have studied the dynamics of spin chains for various model Hamiltonians and found some interesting generic interrelationships between bipartite quantum correlations and information scrambling. We start with a simple initial state, an entangled pair at the first two qubits, and then let the system evolve unitarily. The bipartite quantum correlations have been calculated to show how the information coded in the first two sites as a form of quantum correlation spreads out to other locations. We have shown that the spreading of quantum correlations takes place when the dynamics is restricted to a subspace of the full Hilbert space. In the cases of the Heisenberg model, the transverse field XY model with a very large transverse field and the kicked Harper model, where the number of down (up) spins is a conserved quantity, the entanglement spreads consistently to other parts of the system. On the other hand, for the XY model and the Ising model with a small and moderate transverse field ($|h| < 1$), where the dynamics is spin non-conserving, the

Spin-models	Spin conserving	Integrable	Sign of TMI	Finite speed of correlation propagation
Heisenberg model	yes	yes	non-negative	yes
Transverse field XY model ($\|h\| << J_x, J_y$)	no	yes	negative	no
Transverse field XY model ($h >> J_x, J_y$)	yes	yes	non-negative	yes
Ising model	no	yes	negative	no
Kicked Harper model	yes	no	non-negative	yes

Table 1 The sign of the tripartite mutual information and the propagation of bipartite correlations through the spin chain for different model for one-magnon initial states.

propagation or spreading do not take place from the first two entangled sites, although quantum correlations are generated in the system.

This behaviour can be understood from the perspective of quantum information scrambling. If the dynamics is restricted to a spin conserving subspace, scrambling does not take place. We have shown that the Heisenberg model, the kicked Harper model and the transverse field XY model with $|h| >> 1$ do not show any scrambling behaviour for one down-spin states as TMI is always non-negative. In these cases, the bipartite correlations in the system do not delocalize into multiparitite correlations as time evolves. On the other hand, the XY model with a small transverse field ($|h| < 1$), and the Ising model show a scrambling behaviour even with one down (up) spin initial states. We have also seen that quantum integrability does not play any direct role in scrambling the quantum correlations. The kicked Harper model, a nonintegrable model, does not show scrambling behaviour, whereas the XY model with a transverse field, an integrable model shows scrambling behaviour. In these cases, bipartite correlations quickly delocalize into multipartite correlations as time evolves. However, for other initial states that mix different spin sectors, scrambling does take place in spin-conserving dynamics. For example, the Heisenberg dynamics and the kicked Harper dynamics with an initial state with zero and two magnon sectors do show scrambling; though much smaller compared to that of spin non-conserving models. Occurrence of scrambling in a many-body quantum system, therefore, depends fundamentally on two factors: whether the bipartite correlations delocalize with time owing to non spin-conserving dynamics and whether the dynamics mixes different spin sectors.

Our main results are summarized in Table 1. The table gives a clear relationship between the sign of tripartite mutual information and the propagation of bipartite quantum correlations with time. The models where locally encoded bipartite quantum correlations propagate with a finite speed have a non-negative value of TMI. On the other hand, the information is lost and can not propagate in the models with a negative value of TMI.

Acknowledgments. We acknowledge the support of Department of Physics, Indian Institute of Technology, Kanpur, where part of the work was carried out. VS acknowledges the support of Science and Engineering Research Board, through MATRICS scheme.

Data Availability. All data generated or analyzed during this study are available from the authors on reasonable request.

References

[1] S. Bose, Quantum communication through an unmodulated spin chain, Phys. Rev. Lett. 91 (2003) 207901.

[2] V. Subrahmanyam, Entanglement dynamics and quantum-state transport in spin chains, Phys. Rev. A 69 (2004) 034304.

[3] M. Christandl, N. Datta, A. Ekert, A. J. Landahl, Perfect state transfer in quantum spin networks, Phys. Rev. Lett. 92 (2004) 187902.

[4] Z.-M. Wang, M. Byrd, B. Shao, J. Zou, Quantum communication through anisotropic heisenberg xy spin chains, Physics Letters A 373 (6) (2009) 636–643.

[5] V. Subrahmanyam, A. Lakshminarayan, Transport of entanglement through a heisenberg–xy spin chain, Physics Letters A 349 (1) (2006) 164–169.

[6] S. Sachdev, Quantum Phase Transitions, Cambridge University Press, 1999.

[7] P. Jordan, E. Wigner,Über das paulische äquivalenzverbot, Zeitschrift für Physik 47 (9) (1928) 631–651.

[8] E. Lieb, T. Schultz, D. Mattis, Two soluble models of an antiferromagnetic chain, Annals of Physics 16 (3) (1961) 407–466.

[9] M. Takahashi, Thermodynamics of One-dimensional Solvable models, Cambridge University Press, 2005.

[10] H. Bethe, Zeitschrift für Physik 71 (3) (1931) 205–226.

[11] M. Ganahl, E. Rabel, F. H. L. Essler, H. G. Evertz, Observation of complex bound states in the spin-1/2 heisenberg xxz chain using local quantum quenches, Phys. Rev. Lett. 108 (2012) 077206.

[12] T. Fukuhara, P. Schauß, M. Endres, S. Hild, M. Cheneau, I. Bloch, C. Gross, Microscopic observation of magnon bound states and their dynamics, Nature 502 (7469) (2013) 76–79.

[13] R. Vlijm, M. Ganahl, D. Fioretto, M. Brockmann, M. Haque, H. G. Evertz, J.-S. Caux, Quasi-soliton scattering in quantum spin chains, Phys. Rev. B 92 (2015) 214427.

[14] R. Steinigeweg, S. Langer, F. Heidrich-Meisner, I. P. McCulloch, W. Brenig, Coherent spin-current oscillations in transverse magnetic fields, Phys. Rev. Lett. 106 (2011) 160602.

[15] M. S. Foster, T. C. Berkelbach, D. R. Reichman, E. A. Yuzbashyan, Quantum quench spectroscopy of a luttinger liquid: Ultrarelativistic density wave dynamics due to fractionalization in an xxz chain, Phys. Rev. B 84 (2011) 085146.

[16] M. A. Cazalilla, M.-C. Chung, Quantum quenches in the luttinger model and its close relatives, Journal of Statistical Mechanics: Theory and Experiment 2016 (06) (2016) 064004.

[17] V. Mukherjee, U. Divakaran, A. Dutta, D. Sen, Quenching dynamics of a quantum xy spin-$\frac{1}{2}$ chain in a transverse field, Phys. Rev. B 76 (2007) 174303.

[18] T. Nag, A. Dutta, A. Patra, Quenching dynamics and quantum information, International Journal of Modern Physics B 27 (2013) 1345036.

[19] S. R. Manmana, S. Wessel, R. M. Noack, A. Muramatsu, Time evolution of correlations in strongly interacting fermions after a quantum quench, Phys. Rev. B 79 (2009) 155104.

[20] P. Sodano, A. Bayat, S. Bose, Kondo cloud mediated long-range entanglement after local quench in a spin chain, Phys. Rev. B 81 (2010) 100412.

[21] G. D. Chiara, S. Montangero, P. Calabrese, R. Fazio, Entanglement entropy dynamics of heisenberg chains, Journal of Statistical Mechanics: Theory and Experiment 2006 (03) (2006) P03001–P03001.

[22] A. Safavi-Naini, M. L. Wall, O. L. Acevedo, A. M. Rey, and R. M. Nandkishore, Quantum dynamics of disordered spin chains with power-law interactions, Phys. Rev. A 99 (2019)

[23] Wojciech De Roeck and François Huveneers, Stability and instability towards delocalization in many-body localization systems, Phys. Rev. B 95 (2017)

[24] P. Hayden, J. Preskill, Black holes as mirrors: quantum information in random subsystems, Journal of High Energy Physics 2007 (09) (2007) 120–120.

[25] Y. Sekino, L. Susskind, Fast scramblers, Journal of High Energy Physics 2008 (10) (2008) 065–065.

[26] T. M. Cover, J. A. Thomas, Elements of Information Theory, John Wiley & Sons, 2006.

[27] E. Iyoda, T. Sagawa, Scrambling of quantum information in quantum many-body systems, Phys. Rev. A 97 (2018) 042330.

[28] M. Campisi, J. Goold, Thermodynamics of quantum information scrambling, Phys. Rev. E 95 (2017) 062127.

[29] K. A. Landsman, C. Figgatt, T. Schuster, N. M. Linke, B. Yoshida, N. Y. Yao, C. Monroe, Verified quantum information scrambling, Nature 567 (7746) (2019) 61–65.

[30] A. Seshadri, V. Madhok, A. Lakshminarayan, Tripartite mutual information, entanglement, and scrambling in permutation symmetric systems with an application to quantum chaos, Phys. Rev. E 98 (2018) 052205.

[31] P. Hosur, X.-L. Qi, D. A. Roberts, B. Yoshida, Chaos in quantum channels, Journal of High Energy Physics 2016 (2) (2016) 4.

[32] N. J. Cerf, C. Adami, Information theory of quantum entanglement and measurement, Physica D: Nonlinear Phenomena 120 (1) (1998) 62–81, proceedings of the Fourth Workshop on Physics and Consumption.

[33] V. Subrahmanyam, Quantum entanglement in heisenberg antiferromagnets, Phys. Rev. A 69 (2004) 022311.

[34] W. K. Wootters, Entanglement of formation of an arbitrary state of two qubits, Phys. Rev. Lett. 80 (1998) 2245–2248.

[35] A. Kundu, V. Subrahmanyam, Distribution of quantum correlations and conditional entropy in Heisenberg spin chains, Journal of Physics A: Mathematical and Theoretical 46 (43) (2013) 435304.

[36] S. Sur, V. Subrahmanyam, Remotely detecting the signal of a local decohering process in spin chains, Journal of Physics A: Mathematical and Theoretical 50 (20) (2017) 205303.

[37] S. Sur, V. Subrahmanyam, Interference of the signal from a local dynamical process with the quantum state propagation in spin chains, Journal of Physics A: Mathematical and Theoretical 52 (1) (2018) 015302.

[38] Y. A. Izyumov, Y. N. Skryabin, Statistical Mechanics of Magnetically Ordered Systems, Springer-Verlag, Heidelberg, 1988.

[39] R. Lima, D. Shepelyansky, Fast delocalization in a model of quantum kicked rotator, Phys. Rev. Lett. 67 (1991) 1377–1380.

[40] A. Lakshminarayan, V. Subrahmanyam, Entanglement sharing in one-particle states, Phys. Rev. A 67 (2003) 052304.

[41] S. Sur, A. Ghosh, Quantum counterpart of measure synchronization: A study on a pair of harper systems, Physics Letters A 384 (8) (2020) 126176.

[42] N. N. Bogoljubov, On a new method in the theory of superconductivity, Nuovo Cimento 7 (6) (1958) 794.

[43] J. G. Valatin, Comments on the theory of superconductivity, Nuovo Cimento 7 (6) (1958) 843.

[44] M. E. Peskin, D. V. Schroeder, An introduction to Quantum Field Theory, Persesus Books, Massachusetts, 1995.

[45] I. Lindgren, J. Morrison, Atomic Many-Body Theory, Springer-Verlag, Heidelberg, 1982.

Appendix A Pairwise correlation functions for the XY model with transverse field

The expectation values of the correlation functions $\langle c_j^\dagger c_j\rangle$, $\langle c_j c_{j+1}^\dagger\rangle$, $\langle c_j c_{j+1}\rangle$ and $\langle c_j^\dagger c_j c_{j+1}^\dagger c_{j+1}\rangle$ as a function of time can be calculated analytically as shown as,

$$\begin{aligned}
\langle c_j^\dagger c_j\rangle_t &= \frac{1}{N}\sum_{q_1,q_2} e^{iq_1 j - iq_2 j}\langle(\chi_{q_1}^* c_{q_1}^\dagger + \xi_{q_1}^* c_{-q_1})(\chi_{q_2} c_{q_2} + \xi_{q_2} c_{-q_2}^\dagger)\rangle,\\
\langle c_j c_{j+1}\rangle_t &= \frac{1}{N}\sum_{q_1,q_2} e^{iq_1 j - iq_2 (j+1)}\langle(\chi_{q_1} c_{q_1} + \xi_{q_1} c_{-q_1}^\dagger)(\chi_{q_2} c_{q_2} + \xi_{q_2} c_{-q_2}^\dagger)\rangle,\\
\langle c_j c_{j+1}^\dagger\rangle_t &= \frac{1}{N}\sum_{q_1,q_2} e^{-iq_1 j + iq_2 (j+1)}\langle(\chi_{q_1} c_{q_1} + \xi_{q_1} c_{-q_1}^\dagger)(\chi_{q_2}^* c_{q_2}^\dagger + \xi_{q_2}^* c_{-q_2})\rangle,\\
\langle c_j^\dagger c_j c_{j+1}^\dagger c_{j+1}\rangle_t &= \frac{1}{N^2}\sum_{q_1,q_2,q_3,q_4} e^{iq_1 j - iq_2 j + iq_3 (j+1) - iq_4 (j+1)}\langle(\chi_{q_1}^* c_{q_1}^\dagger + \xi_{q_1}^* c_{-q_1})\\
&\qquad (\chi_{q_2} c_{q_2} + \xi_{q_2} c_{-q_2}^\dagger)(\chi_{q_3}^* c_{q_3}^\dagger + \xi_{q_3}^* c_{-q_3})(\chi_{q_4} c_{q_4} + \xi_{q_4} c_{-q_4}^\dagger)\rangle.
\end{aligned} \tag{A1}$$

We see from the above set of equations that the time evolution mixes the different operators. Any product of fermion operators in the real space involves N sums over momenta values in real space. The expectation values of products of fermionic operators can be straightforwardly evaluated using Wick's theorem [44, 45]. However, there will be N sums over the momentum variables. For a large value of N, the above sums are evaluated by converting them to integrals from 0 to π. The pairwise correlation functions between the nearest neighbours are plotted as functions of site index i and time t in Fig. A1. We have taken three sets of Hamiltonian parameters ($J_x = 0.7, J_y = 0.3, h = 0.1$); ($J_x = 0.7, J_y = 0.3, h = 1.0$) and ($J_x = 0.7, J_y = 0.3, h = 10.0$) to illustrate the results. The total number of down (up) spins in the system is not conserved as $J_x \neq J_y$. However, in the limit $h \to \infty$, the dynamics is confined to a subspace of the total Hilbert space, as the Hamiltonian in this case commutes with the total number of down (up) spins. The initial

state being $|\Psi\rangle = \frac{1}{\sqrt{2}}(100...0 + 010...0)$, the initial values of the off-diagonal correlation function $\langle\sigma_i^+\sigma_{i+1}^-\rangle$ is 0.5 the diagonal correlation function $\langle\sigma_i^z\sigma_{i+1}^z\rangle$ is -1 for the first pair and zero for all other pairs.

As time evolves, the correlation function $\langle\sigma_i^+\sigma_{i+1}^-\rangle$ becomes non zero for farther sites for later times implying a finite speed of propagation of correlations) for the case $h = 0.1$ as shown in Fig. A1(a). The value of the function $\langle\sigma_i^+\sigma_{i+1}^-\rangle$ is non zero within the 'light cone' but zero outside. For the case $h = 1.0$, the correlation function $\langle\sigma_i^+\sigma_{i+1}^-\rangle$ decays very quickly and becomes zero beyond the third site as shown in Fig. A1(b). For the case $h = 10.0$, the correlations propagate consistently and continuously to further sites with a finite speed as shown in Fig. A1(c). The diagonal correlation function $\langle\sigma_i^z\sigma_{i+1}^z\rangle$ becomes non zero for farther sites quickly and propagation does not take place with a finite speed for the cases $h = 0.1$ and $h = 1.0$ as shown in Fig. A1(d) and Fig. A1(e) respectively. For the case $h = 10.0$, the value of the function $\langle\sigma_i^z\sigma_{i+1}^z\rangle$ spreads with finite speed and its value is zero outside the light cone as shown Fig. A1(f). The correlation function $\langle\sigma_i^+\sigma_{i+1}^+\rangle$ is plotted as a function of time and site index for the same set of Hamiltonian parameters in Fig. A1(g), (h) and (i) respectively. The expectation value of the correlation function $\langle\sigma_i^+\sigma_{i+1}^+\rangle$ is initially zero and becomes non zero as the number of down spins increases in the system. The values of $\langle\sigma_i^+\sigma_{i+1}^+\rangle$ for the case $h = 10.0$ in Fig. A1(i) is much smaller compared to the cases $h = 0.1$ and $h = 1.0$ as seen in Fig. A1(g) and Fig. A1(h) respectively. This indicates that for a high value of h, less number of down spins are generated in the system as time evolves and the dynamics remains confined mainly in the one spin sector.

Appendix B Pairwise correlation functions for the Ising model

For the Ising model the time evolved expectation value of any operator O is given as

$$\langle O\rangle_t = \langle e^{iJt\sum_i \sigma_i^x\sigma_{i+1}^x} O e^{-iJt\sum_i \sigma_i^x\sigma_{i+1}^x}\rangle. \tag{B1}$$

The forms of $\langle\sigma_j^z\rangle_t, \langle\sigma_j^\pm\rangle_t, \langle\sigma_j^z\sigma_{j+1}^z\rangle_t$ and $\langle\sigma_j^+\sigma_{j+1}^\mp\rangle_t$ can be given by the following,

$$\begin{aligned}
\langle\sigma_j^z\rangle_t &= (C^4 + S^4 - 2C^2S^2)\langle\sigma_j^z\rangle + (2CS^3 - 2C^3S)(\langle\sigma_j^y\sigma_{j+1}^x\rangle + \langle\sigma_{j-1}^x\sigma_j^y\rangle) \\
&\quad - 4C^2S^2\langle\sigma_{j-1}^x\sigma_j^z\sigma_{j+1}^x\rangle, \\
\langle\sigma_j^\pm\rangle_t &= 0, \\
\langle\sigma_j^z\sigma_{j+1}^z\rangle_t &= (C^6 + S^6 - C^4S^2 - C^2S^4)\langle\sigma_j^z\sigma_{j+1}^z\rangle + (CS^5 + C^3S^3 - 2C^5S)(\langle\sigma_j^z\sigma_{j+1}^y\sigma_{j+2}^x\rangle \\
&\quad + \langle\sigma_{j-1}^x\sigma_j^y\sigma_{j+1}^z\rangle) + (4C^2S^4 + 4C^4S^2)\langle\sigma_{j-1}^x\sigma_j^y\sigma_{j+1}^y\sigma_{j+2}^x\rangle, \\
\langle\sigma_j^+\sigma_{j+1}^\mp\rangle_t &= (C^6 + S^6)\langle\sigma_j^+\sigma_{j+1}^\mp\rangle + (C^4S^2 + C^2S^4)(\langle\sigma_j^+\sigma_{j+1}^\pm\rangle + \langle\sigma_j^-\sigma_{j+1}^\pm\rangle + \langle\sigma_j^-\sigma_{j+1}^\mp\rangle)
\end{aligned}$$

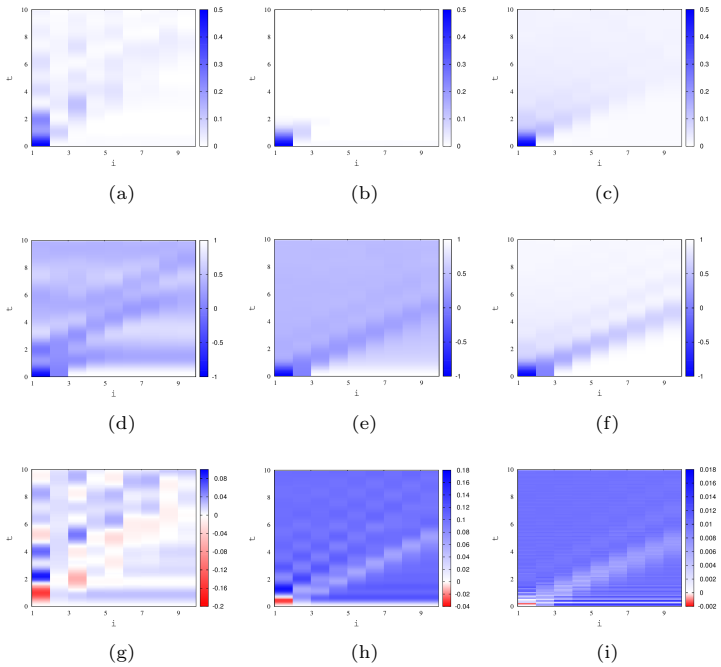


Fig. A1 The correlation functions between the sites i and $i+1$ are shown as functions of time t for the transverse field XY model for various Hamiltonian parameters. $\mathrm{Re}\langle\sigma_i^+\sigma_{i+1}^-\rangle_t$ is plotted as a function of time for parameters: (a) $J_x = 0.7, J_y = 0.3$ and $h = 0.1$, (b) $J_x = 0.7, J_y = 0.3$ and $h = 1.0$, (c) $J_x = 0.7, J_y = 0.3$ and $h = 10.0$. $\mathrm{Re}\langle\sigma_i^+\sigma_{i+1}^+\rangle_t$ is plotted as a function of time for parameters: (d) $J_x = 0.7, J_y = 0.3$ and $h = 0.1$, (e) $J_x = 0.7, J_y = 0.3$ and $h = 1.0$, (f) $J_x = 0.7, J_y = 0.3$ and $h = 10.0$. $\langle\sigma_i^z\sigma_{i+1}^z\rangle_t$ for parameters: (g) $J_x = 0.7, J_y = 0.3$ and $h = 0.1$, (h) $J_x = 0.7, J_y = 0.3$ and $h = 1.0$, (i) $J_x = 0.7, J_y = 0.3$ and $h = 10.0$. The results are shown from analytical calculations for the initial state: $|\Psi(0)\rangle = (|10...0\rangle + |010...0\rangle)/\sqrt{2}$.

$$
\begin{aligned}
&+(iC^5S - iC^3S^3)\Big(\frac{1}{2}\langle\sigma_j^+(1\mp\sigma_{j+1}^z)\sigma_{j+2}^x\rangle + \frac{1}{2}\langle\sigma_{j-1}^x(1+\sigma_j^z)\sigma_{j+1}^{\mp}\rangle + \frac{1}{4}(1+\sigma_j^z)(1\mp\sigma_{j+1}^z)\Big)\\
&+(iCS^5 - iC^5S)\Big(\frac{1}{2}\langle\sigma_j^+(1\pm\sigma_{j+1}^z)\sigma_{j+2}^x\rangle + \frac{1}{2}\langle\sigma_{j-1}^x(1-\sigma_{j+1}^z)\sigma_{j+1}^{\mp}\rangle + \frac{1}{4}(1-\sigma_j^z)(1\pm\sigma_{j+1}^z)\\
&+(C^2S^4 + C^4S^2)\Big(\frac{1}{4}\langle\sigma_{j-1}^x(1+\sigma_j^z)(1\pm\sigma_{j+1}^z)\sigma_{j+2}^x\rangle - \frac{1}{4}\langle\sigma_{j-1}^x(1-\sigma_j^z)(1\pm\sigma_{j+1}^z)\sigma_{j+2}^x\rangle\\
&-\frac{1}{4}\langle\sigma_{j-1}^x(1+\sigma_j^z)(1\mp\sigma_{j+1}^z)\sigma_{j+2}^x\rangle + \frac{1}{4}\langle\sigma_{j-1}^x(1-\sigma_j^z)(1\mp\sigma_{j+1}^z)\sigma_{j+2}^x\rangle\\
&+\frac{1}{2}\langle\sigma_{j-1}^x\sigma_j^-(1\mp\sigma_{j+1}^z)\rangle + \frac{1}{2}\langle\sigma_{j-1}^x\sigma_j^-(1\pm\sigma_{j+1}^z)\rangle - \frac{1}{2}\langle\sigma_{j-1}^x\sigma_j^+(1\pm\sigma_{j+1}^z)\rangle\\
&-\frac{1}{2}\langle\sigma_{j-1}^x\sigma_j^+(1\mp\sigma_{j+1}^z)\rangle\Big) + \frac{1}{2}\langle(1+\sigma_j^z)\sigma_{j+1}^{\pm}\sigma_{j+2}^x\rangle + \frac{1}{2}\langle(1+\sigma_j^z)\sigma_{j+1}^{\pm}\sigma_{j+2}^x\rangle\\
&-\frac{1}{2}\langle(1-\sigma_j^z)\sigma_{j+1}^{\pm}\sigma_{j+2}^x\rangle - \frac{1}{2}\langle(1+\sigma_j^z)\sigma_{j+1}^{\pm}\sigma_{j+2}^x\rangle\Big),
\end{aligned}
\tag{B2}
$$

with, $C \equiv \cos(Jt)$ and $S \equiv \sin(Jt)$.